Title

Tuning interfacial exchange interactions via electronic reconstruction in transition-metal oxide heterostructures

Journal

Applied Physics Letters, 109(15)

ISSN

0003-6951

Authors

Li, Binzhi
Chopdekar, Rajesh V
N'Diaye, Alpha T
et al.

Publication Date

2016-10-10

DOI

10.1063/1.4964407

Peer reviewed

AIP | Applied Physics Letters

Tuning interfacial exchange interactions via electronic reconstruction in transition-metal oxide heterostructures

Binzhi Li, Rajesh V. Chopdekar, Alpha T. N'Diaye, Apurva Mehta, J. Paige Byers, Nigel D. Browning, Elke Arenholz, and Yayoi Takamura

Citation: Applied Physics Letters **109**, 152401 (2016); doi: 10.1063/1.4964407
View online: http://dx.doi.org/10.1063/1.4964407
View Table of Contents: http://scitation.aip.org/content/aip/journal/apl/109/15?ver=pdfcov
Published by the AIP Publishing

Tuning interfacial exchange interactions via electronic reconstruction in transition-metal oxide heterostructures

Binzhi Li,[1] Rajesh V. Chopdekar,[1] Alpha T. N'Diaye,[2] Apurva Mehta,[3] J. Paige Byers,[1] Nigel D. Browning,[4] Elke Arenholz,[2] and Yayoi Takamura[1,a)]
[1]*Department of Materials Science and Engineering, University of California, Davis, One Shields Ave, Davis, California 95616, USA*
[2]*Advanced Light Source, Lawrence Berkeley National Laboratory, 1 Cyclotron Rd., Berkeley, California 94720, USA*
[3]*Stanford Synchrotron Radiation Lightsource, SLAC National Accelerator Laboratory, Menlo Park, California 94025, USA*
[4]*Physical and Computational Science Directorate, Pacific Northwest National Laboratory, Richland, Washington 99354, USA*

(Received 27 June 2016; accepted 24 September 2016; published online 10 October 2016)

The impact of interfacial electronic reconstruction on the magnetic characteristics of $La_{0.7}Sr_{0.3}CoO_3$ (LSCO)/$La_{0.7}Sr_{0.3}MnO_3$ (LSMO) heterostructures was investigated as a function of layer thickness using a combination of soft x-ray magnetic spectroscopy and bulk magnetometry. We found that the magnetic properties of the LSCO layers are impacted by two competing electronic interactions occurring at the LSCO/substrate and LSMO/LSCO interfaces. For thin LSCO layers (<5 nm), the heterostructures exist in a highly coupled state where the chemically distinct layers behave as a single magnetic compound with magnetically active Co^{2+} ions. As the LSCO thickness increases, a high coercivity LSCO layer develops which biases a low coercivity layer, which is composed not only of the LSMO layer but also an interfacial LSCO layer. These results suggest an intriguing route to tune the magnetic properties of transition metal oxide heterostructures through careful control of the interface structure. *Published by AIP Publishing.* [http://dx.doi.org/10.1063/1.4964407]

Recent advances in thin film growth technology with atomic-level precision have enabled the discovery of a wide range of fascinating physical phenomena at interfaces in transition-metal oxide (TMO) heterostructures.[1] These phenomena arise from the complex interactions between the lattice, charge, spin, and orbital degrees of freedom that are highly sensitive to external stimuli such as strain, chemical doping, and electric and magnetic fields.[2] TMO heterostructures consisting of layers with competing magnetic characteristics have attracted attention from a fundamental perspective[3] as well as their potential applications in magnetic sensors, magnetic random access memory, and spintronics devices.[4] In magnetic TMO heterostructures, interfaces can possess unique characteristics that are not found in the individual constituent materials due to effects such as interfacial charge transfer, strain due to lattice mismatch, and magnetic reconstruction. These interface phases can lead to intriguing interfacial exchange interactions, such as exchange bias (EB)[5,6] at interfaces that do not involve antiferromagnetic and ferromagnetic (FM) layers. For example, Gibert *et al.*[7] reported an EB effect in heterostructures composed of paramagnetic (PM) $LaNiO_3$ and FM $LaMnO_3$ layers. Similarly, heterostructures composed of soft and hard FM layers can exhibit EB effects characterized by a unidirectional magnetic anisotropy induced by exchange interactions.[8–11]

The aim of this work is to perform a detailed investigation into the magnetic spin/electronic structures, which develop at interfaces in $La_{0.7}Sr_{0.3}MnO_3$ (LSMO)/$La_{0.7}Sr_{0.3}CoO_3$ (LSCO) heterostructures grown on $(LaAlO_3)_{0.3}(Sr_2AlTaO_6)_{0.7}$ (LSAT) substrates. LSMO is a soft FM metal that shows coincident FM-to-PM and metal-to-insulator transitions at ~360 K.[12,13] In bulk form, $La_{1-x}Sr_xCoO_3$ with $x < 0.22$ displays magneto-electronic phase separation (MEPS),[14–16] where FM/metallic clusters are embedded in a non-magnetic/insulating matrix. At higher Sr doping, the FM clusters form a percolation network, which displays long-range FM/metallic behavior. MEPS occurs in $La_{1-x}Sr_xCoO_3$ thin films when the thickness is reduced below a critical value (~8 nm), even when the bulk composition displays strong FM behavior.[15] Such MEPS was ascribed to local chemical inhomogeneity such as oxygen deficiency at the film/substrate interface. Here, we show that by decreasing the LSCO layer thickness in the LSMO/LSCO heterostructures, the MEPS phenomenon at the LSCO/LSAT interface competes with a second type of magneto-electronic interaction at the LSCO/LSMO interface, which is characterized by magnetically active Co^{2+} ions. The competition between these two interfacial effects provides a route to tune the magnetic properties of the heterostructures.

Epitaxial LSCO/LSMO heterostructures were grown on (001)-oriented LSAT substrates by pulsed laser deposition using a KrF excimer laser ($\lambda = 248$ nm). During growth, the substrate temperature was held at 700 °C, the oxygen pressure was 0.3 Torr, and a laser energy of 1.2 J/cm^2 with 5 Hz frequency was used. To ensure proper oxygen stoichiometry, the samples were cooled slowly in 300 Torr oxygen pressure. The LSCO layers were grown first with thicknesses of 2 nm (5 unit cells (uc)), 4 nm (10 uc), and 8 nm (20 uc), followed by a fixed LSMO thickness of 6 nm (15 uc). Samples were denoted as CM2, CM4, and CM8, respectively. Thicker heterostructures (CM17) consisting of 17 nm LSCO/20 nm LSMO were also grown.

The structural properties of the heterostructures were characterized using x-ray reflectivity (XRR), high-resolution x-ray diffraction, and reciprocal space maps (RSMs) taken with a

a)E-mail: ytakamura@ucdavis.edu

Bruker D8 Discover 4-circle diffractometer and at beamline 2-1 at the Stanford Synchrotron Radiation Lightsource (SSRL, Figs. S1–S3 of the supplementary material), as well as scanning transmission electron microscopy (STEM, Fig. S4 of the supplementary material). The ω-2θ scans show the presence of (002) diffraction peaks and Kiessig fringes revealing highly crystalline, single-phase layers of LSMO and LSCO in the heterostructures. The thickness, density, and roughness of the layers were determined by fitting the XRR spectra using the GENX program, which reveal chemically distinct LSMO and LSCO layers with little intermixing (~1 uc).[17] The fitted thicknesses are tabulated in Tables SI–SIII (supplementary material). RSMs around the (103) peaks show fully epitaxial growth of both layers on the (001)-oriented LSAT substrate, where the LSMO and LSCO layers are under compressive and tensile strain, respectively. The STEM images (Fig. S4 of the supplementary material) further confirm the high structural quality of the epitaxial LSMO/LSCO heterostructures with sharp interfaces and few structural defects.

The magnetic switching behavior was characterized using bulk magnetometry and x-ray magnetic circular dichroism (XMCD) spectroscopy at 80 K. Bulk magnetization was studied using a Quantum Design superconducting quantum interference device (SQUID) magnetometer with the magnetic field applied along the in-plane [100] substrate direction. The linear contribution from the diamagnetic LSAT substrate was subtracted from the data, and the magnetization was normalized to the sample surface area. X-ray absorption (XA) and XMCD spectra provide element-specific characterization of the electronic structure and magnetization process in the different layers, respectively. XA/XMCD spectra were acquired on beamlines 6.3.1 and 4.0.2 of the Advanced Light Source (ALS) in total-electron-yield (TEY) and luminescence yield (LY) modes. TEY mode provides surface sensitive information limited by the finite escape depth of secondary electrons (5–10 nm) and therefore provides average information for the entire LSMO layer, though weighted towards the surface region, and only detects the LSCO layer near the LSMO/LSCO interface. In LY detection, the x-rays transmit through the sample, thus providing average information from the entire LSMO and LSCO layers.[18] A linear background was subtracted from the LY data, and all curves were normalized to the peak value. The applied magnetic field direction was collinear with the x-ray beam that impinged on the sample surface at 60° to the surface normal.

The magnetic properties of samples CM2 and CM4 with the thinner LSCO layers are plotted in Figures 1 and S5 (supplementary material). Despite the fact that the resonant XRR spectra confirm that there are two chemically distinct layers, a single switching event is observed in the SQUID hysteresis loops with a small coercivity similar to that of an LSMO film (0.005 T for LSMO, 0.012 T for CM2, and 0.023 T for CM4). The Co- and Mn-XMCD loops (Fig. 1(b) and S5(b) (supplementary material)) probe the magnetic switching of the two layers independently and were obtained by tuning the x-ray photon energy to the Co/Mn L edges with maximum XMCD signal. These loops match one another exactly, signaling the presence of a magnetically "soft" LSCO layer, which is magnetically coupled to the LSMO layer, with a lack of a magnetically hard LSCO layer. The areal magnetization remains nearly constant for samples CM2 and CM4 despite the difference in LSCO layer thickness, suggesting the formation of a non-magnetic layer at the LSAT interface as has been reported for LSCO films on other substrates.[14–16]

Upon increasing the LSCO layers thickness (i.e., sample CM8), a different magnetic switching behavior develops. Fig. 2(a) plots the major hysteresis loop measured by SQUID magnetometry with a maximum field of 2.0 T, and it shows the expected two-step magnetic transition for composite materials with components of different coercivities. The magnetic transitions at 0.002 T and 0.6 T correspond well with the coercivity of the soft LSMO and hard LSCO layers, respectively.[8] In order to investigate the exchange interactions between the two layers, minor loops were measured where the samples were first biased at ±1.8 T to reach full saturation, and then loops were measured between ±0.2 T. This smaller field induces switching only in the soft layer. The biased minor loops (Fig. 2(b)) show two major features: (1) vertical shift along the magnetization axis and (2) lateral shift along the field axis. The vertical shift is attributed to the magnetization of the hard LSCO layer, which remains magnetized along the direction of the initial biasing field. The lateral shift (~0.007 T) is always in the direction opposite to the biasing field, whereby the magnetic moment of the LSMO layer is pinned by the underlying LSCO layer. These results provide direct evidence of FM exchange interactions at the LSMO/LSCO interface similar to EB effects at FM/AFM interfaces.[8] This EB-behavior persists in sample CM17 with much thicker layers.

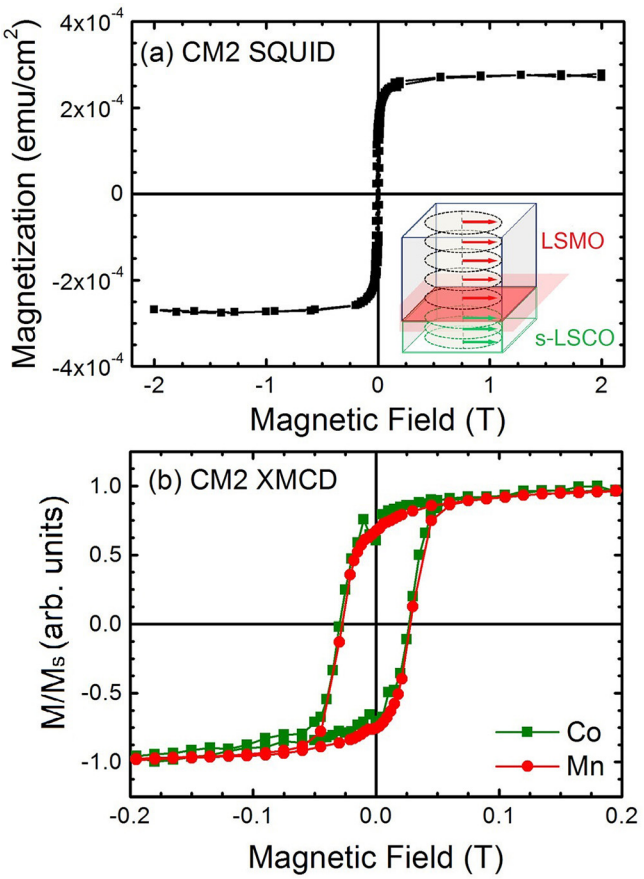

FIG. 1. Hysteresis loops for sample CM2 measured by (a) SQUID magnetometry and (b) XMCD. The inset in (a) shows a schematic of the magnetic layers in sample CM2.

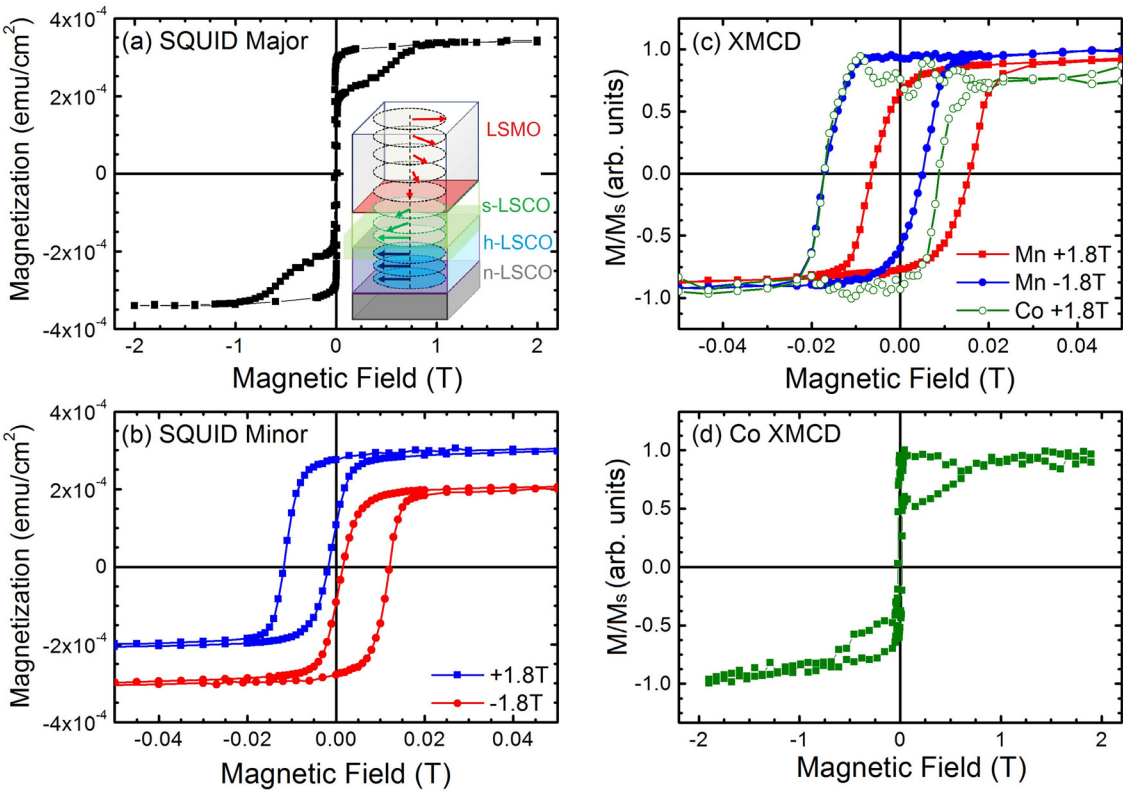

FIG. 2. Hysteresis loops for sample CM8 measured by SQUID magnetometry: (a) major loop and (b) biased minor loops. (c) Biased XMCD minor loops and (d) Co-XMCD major loop measured in the TEY mode. The inset in (a) shows a schematic of the magnetic layers in sample CM8.

The same biasing scheme was employed with the XMCD hysteresis loops. Mn-XMCD minor loops (Fig. 2(c)) show a similar shift along the magnetic field axis as observed from the SQUID measurements, with the direction of the shift in the opposite direction of the biasing field. This result confirms that the LSMO moments are pinned at the interface by the hard LSCO layer due to exchange interactions. Surprisingly, the Co-XMCD major loop (Fig. 2(d)) displays a two-step magnetic transition, contrary to what one would expect from a single phase LSCO film. The transition fields of 0.002 T and 0.6 T agree well with the values obtained from SQUID measurements. Biased Co-XMCD minor loops (Fig. 2(c)) match well with the Mn-XMCD loops in terms of the magnitude of the shift as well as the overall loop profile. These findings indicate that the LSCO layer is composed of two magnetic phases, the expected magnetically hard phase and a soft phase strongly coupled to the LSMO layer.[8]

To understand the physical origin of the interfacial exchange interactions, the electronic structure of the heterostructures were investigated using XA/XMCD spectroscopy. Co/Mn *L*-edge XA spectra involve excitation of electrons from filled 2p to empty 3d states, and provide information on valence states and bonding environments of transition metal ions. XA spectra were determined as the average of spectra taken with right circularly polarized x-rays with H = ±0.2 T or 1.8 T. Mn-XA spectra for the heterostructures (Fig. S6 of the supplementary material) show subtle differences compared to an LSMO thin film: the Mn L_3 peak for the heterostructures displays a shoulder feature 2.2 eV below the main peak, while the feature 1.6 eV below the main peak is less pronounced. These features are associated with an increase in Mn^{4+}/Mn^{3+} ratio in the LSMO layer, presumably localized to the region near the LSMO/LSCO interface.[19–23] Mn-XMCD spectra resemble that of an LSMO thin film in terms of line shape and magnitude, consistent with the small concentration dependence of the magnetic properties of $La_{1-x}Sr_xMnO_3$ for $0.2 < x < 0.4$.[12]

Due to the surface sensitivity of the Co-XA spectra measured in the TEY mode (Fig. 3(a)), these spectra are most sensitive to the valence states of Co ions at the LSMO/LSCO interface, in contrast to LY mode (Fig. 3(b)), which provides information averaged through the entire film thickness. Co-line shapes were compared to LSCO films (2 nm and 36 nm thickness), which nominally have mixed Co^{3+}/Co^{4+} valence states (characterized by feature D in Fig. 3(a)) and a $CoFe_2O_4$ thin film (50 nm thickness) in which the Co^{2+} ions predominantly occupy octahedral sites in the spinel structure.[24] For both detection modes, a clear dependence of the Co multiplet structure at the L_3 edge on the LSCO layer thickness was observed. The Co-XA spectrum for sample CM2 strongly resembles that of $CoFe_2O_4$ showing an unexpected Co^{2+} valence state (features A, B, and C). In contrast, the XA spectra for a 2 nm thick LSCO film more closely resembles Co^{3+} spectra (feature E and energy shift of feature D to lower photon energy), an effect associated with the LSCO/LSAT interface.[25–27] This result demonstrates that the observed valence state change is dominated by electronic interactions at the LSMO/LSCO interface rather than the LSCO/LSAT interface. For sample CM4, the TEY signal is dominated by Co^{2+} ions with a small contribution from Co^{3+}/Co^{4+} ions, as seen by the presence of features A and B from the Co^{2+} spectra and the relative increase in intensity and width of the peak denoted with "*" due to the overlap of features C and D. At the same time, the LY signal

more closely resembles the LSCO reference spectrum indicating that the Co^{3+}/Co^{4+} ions are located in the heterostructure away from the LSMO/LSCO interface. With increasing LSCO layer thickness, the Co spectra for sample CM8 (both TEY and LY) show signatures mostly from the Co^{3+}/Co^{4+} ions. A small concentration of Co^{2+} ions remains in the sample, presumably at the LSCO/LSMO interface, as indicated by the weak signal from feature A. To provide a quantitative analysis of the electronic structure, the TEY Co-XA L_3 edge spectra of the heterostructures were fit using a linear combination of the spectra for the thick LSCO and $CoFe_2O_4$ films (Fig. S7 of the supplementary material). Furthermore, the layer thicknesses for the different Co valence states can be estimated based on the assumption that there is an electronic phase separation along the thickness direction of the LSCO layer. This analysis (Fig. S8 and Table SIV (supplementary material)) shows that the thickness of the interfacial Co^{2+} layer is on the order of 1–2 nm for all three heterostructures.

Co-XMCD spectra were acquired using magnetic fields of 1.8 T and 0.2 T to extract the magnetic contributions of bulk-like LSCO and interfacial LSCO layers, respectively. For the two thinner heterostructures (CM2 and CM4, Fig. 3(b)), Co-XMCD line profiles closely resemble the $CoFe_2O_4$ spectrum irrespective of the magnetic field confirming that the magnetically active ions are in the Co^{2+} state. These moments are fully saturated at fields below 0.2 T and have a larger magnitude than the LSCO film. The contributions of Co^{3+}/Co^{4+} ions to the XA spectra combined with the lack of magnetic signal from Co^{3+}/Co^{4+} ions in sample CM4 further support the existence of a non-magnetic Co^{3+}/Co^{4+} phase (n-LSCO) at the LSCO/LSAT interface.

For sample CM8, a clear difference in the Co-XMCD spectra taken at 0.2 T and 1.8 T (Fig. 3(d)) highlights the presence of two magnetic LSCO phases. The Co-XMCD spectrum measured at 0.2 T resembles that of $CoFe_2O_4$, indicating that Co^{2+} ions are responsible for the observed soft FM phase (s-LSCO) that switches concurrently with the top LSMO layer. At 1.8 T, an additional contribution can be seen around 780 eV (shaded region). The difference spectrum calculated between Co-XMCD spectra measured at 0.2 T and 1.8 T carries all the features of the LSCO reference, suggesting that the hard LSCO phase (h-LSCO) within the heterostructure preserves the magnetic characteristics of bulk LSCO. An n-LSCO layer is also believed to exist at the substrate interface, but it is difficult to directly confirm using the experimental techniques in this study.

The magnetic and XA results imply a strong correlation between the magnetic spin structure and electronic valence states within the LSCO layer. For sample CM2, the 2 nm LSCO layer consists entirely of the s-LSCO phase with magnetically active Co^{2+} ions exchanged coupled to the LSMO layer. For sample CM4, there is an additional n-LSCO phase with mixed Co^{3+}/Co^{4+} valence below the ~1 to 2 nm thick s-

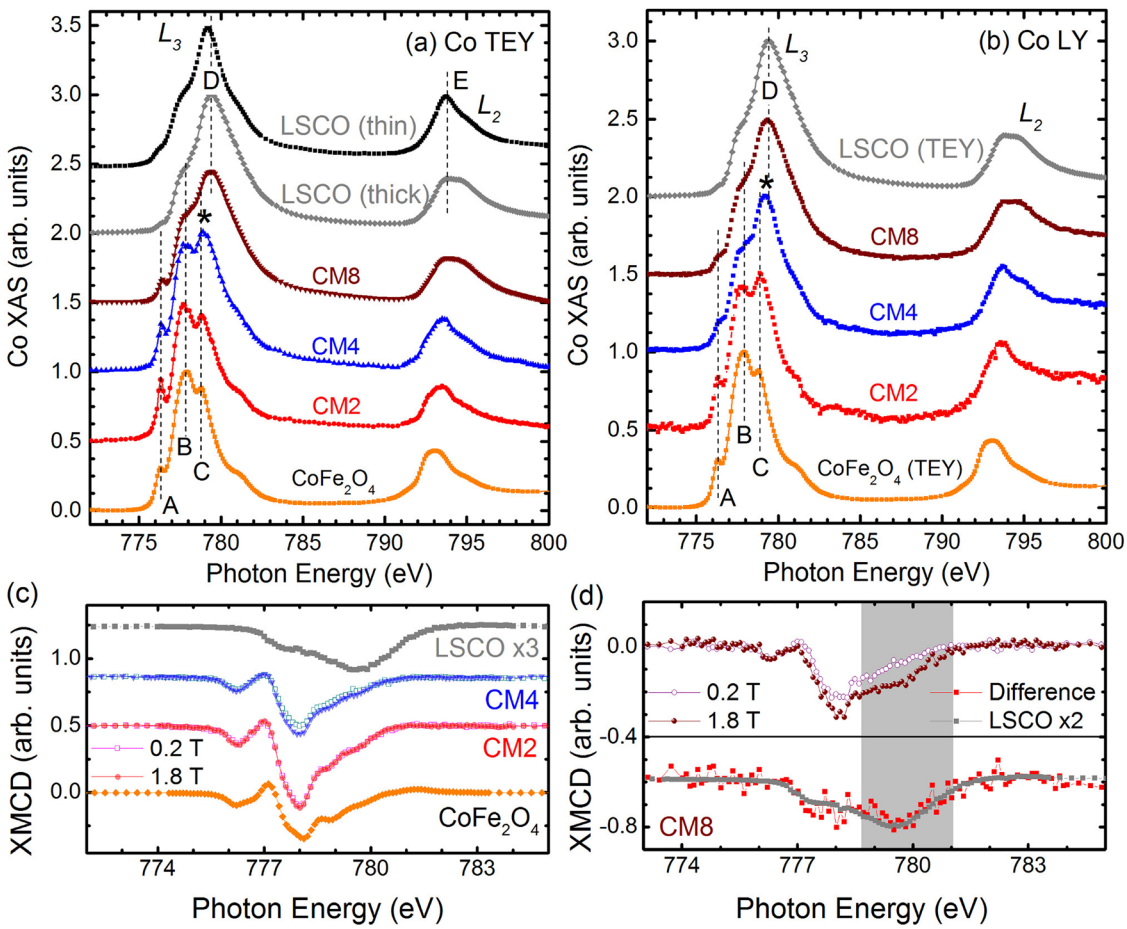

FIG. 3. Co *L*-edge XA spectra taken in (a) TEY mode and (b) LY mode. Labels A-E denote prominent features in the reference spectra for LSCO (2 nm and 36 nm) and $CoFe_2O_4$ thin films (50 nm) taken in the TEY mode. Co-XMCD spectra (L_3 edge only, TEY mode) measured at 0.2 T (open symbols) and 1.8 T (solid symbols) for samples (c) $CoFe_2O_4$, CM2, CM4, and LSCO (x3) and (d) CM8 (top panel). (Bottom panel) Co-XMCD difference calculated from spectra acquired at 0.2 and 1.8 T.

LSCO phase. Finally, sample CM8 is composed of three LSCO phases separated vertically: the n-LSCO phase at the LSCO/LSAT interface, the h-LSCO phase at the interior of the LSCO layer, and the s-LSCO phase at the LSMO/LSCO interface. This model explains the observed two-step magnetic transition in Co-XMCD loops where the first and second transitions correspond to magnetic switching of the interfacial and bottom LSCO layers, respectively. Therefore, the soft/hard FM interface responsible for the EB behavior is located at the interior of the LSCO layer, between the s-LSCO and h-LSCO phases.

These findings allow us to compare the strength of the two competing interfacial phenomena at LSCO/LSMO and LSCO/LSAT interfaces. At the LSCO/LSMO interface, the existence of magnetically active Co^{2+} ions is accompanied by an increased Mn^{4+} concentration in the LSMO layer due to charge transfer in the form of $Mn^{3+} + Co^{3+} \rightarrow Mn^{4+} + Co^{2+}$.[8] The thickness of the s-LSCO layer agrees with the length scale of a few unit cells reported for charge transfer in other perovskite systems such as $SrTiO_3/LaTiO_3$ and $LaMnO_3/SrMnO_3$.[28,29] According to Goodenough-Kanamori-Anderson (GKA) rules,[30] a FM superexchange coupling through Mn^{4+}-O-Co^{2+} chains across the LSCO/LSMO interface is expected, and it is believed to result in the observed concurrent switching behavior between the LSMO and s-LSCO layers. $La_{1-x}Sr_xCoO_3$ thin films have been shown to display modified magnetic and electronic properties at the LSCO/substrate interface for several different substrates.[15,31] This phenomenon was ascribed to MEPS, which was driven by chemical inhomogeneity that subsequently changed the effective hole doping level, and thus favored reduced magnetization. For LSCO layer thickness >5 nm, the LSCO phase separates into three layers through the film thickness, the n-LSCO layer at the LSAT interface, the expected h-LSCO layer at the interior, and the s-LSCO layer at the LSMO/LSCO interface. Interestingly, sample CM2 shows strong magnetization from magnetically active Co^{2+} ions even though the LSCO layer thickness is below the critical thickness for MEPS in LSCO films on LSAT substrates. Therefore, at ultra-thin layer thicknesses, charge transfer at the LSCO/LSMO interface dominates over the substrate-induced MEPS, thereby suppressing the formation of the n-LSCO phase.

In summary, using a combination of bulk magnetometry and soft x-ray magnetic spectroscopy, we have revealed the magnetic and electronic structures of LSMO/LSCO heterostructures as well as their effect on the magnetic switching behavior. The LSCO layer is found to be composed of multiple magnetic and electronic phases separated vertically along the film thickness direction driven by interfacial effects, namely, substrate-induced MEPS at the LSCO/LSAT interface and charge transfer at the LSCO/LSMO interface. In the limit of ultrathin LSCO layers (<5 nm), the competing interfacial interactions lead to an unexpected magnetically-soft LSCO phase with magnetically active Co^{2+} ions. These findings demonstrate the high tunability of the magnetic properties of TMO heterostructures through interface engineering.

See supplementary material for complete structural and magnetic characterization of the LSMO/LSCO heterostructures.

This work was supported by the Semiconductor Research Corporation under Task No. 2309.001. The ALS is supported by the Director, Office of Science, Office of Basic Energy Sciences, of the U.S. Department of Energy (DOE) under Contract No. DE-AC02-05CH11231. Use of the SSRL, SLAC National Accelerator Laboratory, was supported by the U.S. DOE, Office of Science, Office of Basic Energy Sciences, under Contract No. DE-AC02-76SF00515. Some of the research described in this paper is part of the Chemical Imaging Initiative; it was conducted under the Laboratory Directed Research and Development Program at Pacific Northwest National Laboratory (PNNL), a multiprogram national laboratory operated by Battelle for the U.S. DOE under Contract DE-AC05- 76RL01830. A portion of the research was performed using the Environmental Molecular Sciences Laboratory, a national scientific user facility sponsored by the U.S. DOE, Office of Biological and Environmental Research and located at PNNL.

[1]P. Yu, Y.-H. Chu, and R. Ramesh, Mater. Today **15**, 320 (2012).
[2]P. Zubko, S. Gariglio, M. Gabay, P. Ghosez, and J.-M. Triscone, Annu. Rev. Condens. Matter Phys. **2**, 141 (2011).
[3]K. Ueda, H. Tabata, and T. Kawai, Science **280**, 1064 (1998).
[4]M. Bibes, J. E. Villegas, and A. Barthélémy, Adv. Phys. **60**, 5 (2011).
[5]M. Kiwi, J. Magn. Magn. Mater. **234**, 584 (2001).
[6]J. Nogues and I. K. Schuller, J. Magn. Magn. Mater. **192**, 203 (1999).
[7]M. Gibert, P. Zubko, R. Scherwitzl, J. Íñiguez, and J.-M. Triscone, Nat. Mater. **11**, 195 (2012).
[8]B. Li, R. V. Chopdekar, E. Arenholz, A. Mehta, and Y. Takamura, Appl. Phys. Lett. **105**, 202401 (2014).
[9]R. Skomski and J. M. D. Coey, Phys. Rev. B **48**, 15812 (1993).
[10]E. F. Kneller and R. Hawig, IEEE Trans. Magn. **27**, 3588 (1991).
[11]E. E. Fullerton, J. S. Jiang, and S. D. Bader, J. Magn. Magn. Mater. **200**, 392 (1999).
[12]J. Hemberger, A. Krimmel, T. Kurz, H.-A. Krug von Nidda, V. Yu. Ivanov, A. A. Mukhin, A. M. Balbashov, and A. Loidl, Phys. Rev. B **66**, 094410 (2002).
[13]Y. Tokura and Y. Tomioka, J. Magn. Magn. Mater. **200**, 1 (1999).
[14]M. Sharma, J. Gazquez, M. Varela, J. Schmitt, and C. Leighton, Phys. Rev. B **84**, 024417 (2011).
[15]M. A. Torija, M. Sharma, J. Gazquez, M. Varela, C. He, J. Schmitt, J. A. Borchers, M. Laver, S. El-Khatib, and C. Leighton, Adv. Mater. **23**, 2711 (2011).
[16]J. Wu and C. Leighton, Phys. Rev. B **67**, 174408 (2003).
[17]M. Bjorck and G. Andersson, J. Appl. Cryst. **40**, 1174 (2007).
[18]A. Bianconi, D. Jackson, and K. Monahan, Phys. Rev. B **17**, 2021 (1978).
[19]Y. Takamura, F. Yang, N. Kemik, E. Arenholz, M. D. Biegalski, and H. M. Christen, Phys. Rev. B **80**, 180417(R) (2009).
[20]F. M. F. de Groot, J. Electron Spectrosc. **67**, 529 (1994).
[21]J. Hoffman, I. C. Tung, B. B. Nelson-Cheeseman, M. Liu, J. W. Freeland, and A. Bhattacharya, Phys. Rev. B **88**, 144411 (2013).
[22]M. Gu, F. Yang, E. Arenholz, N. D. Browning, and Y. Takamura, J. Magn. Magn. Mater. **325**, 69 (2013).
[23]M. Abbate, F. M. F. de Groot, J. C. Fuggle, A. Fujimori, O. Strebel, F. Lopez, M. Domke, G. Kaindl, G. A. Sawatzky, M. Takano, Y. Takeda, H. Eisaki, and S. Uchida, Phys. Rev. B **46**, 4511 (1992).
[24]R. V. Chopdekar, M. Liberati, Y. Takamura, L. F. Kourkoutis, J. S. Bettinger, B. B. Nelson-Cheeseman, E. Arenholz, A. Doran, A. Scholl, D. A. Muller, and Y. Suzuki, J. Magn. Magn. Mater. **322**, 2915 (2010).
[25]V. K. Malik, C. H. Vo, E. Arenholz, A. Scholl, A. T. Young, and Y. Takamura, J. Appl. Phys. **113**, 153907 (2013).
[26]M. Merz, P. Nagel, C. Pinta, Samartsev, H. v. Lohneysen, M. Wissinger, S. Uebe, A. Assmann, D. Fuchs, and S. Schuppler, Phys. Rev. B **82**, 174416 (2010).
[27]C. Pinta, D. Fuchs, M. Merz, M. Wissinger, E. Arac, H. v. Lohneysen, A. Samartsev, P. Nagel, and S. Schuppler, Phys. Rev. B **78**, 174402 (2008).
[28]A. Ohtomo, D. A. Muller, J. L. Grazul, and H. Y. Hwang, Nature **419**, 378 (2002).
[29]S. Smadici, P. Abbamonte, A. Bhattacharya, X. Zhai, B. Jiang, A. Rusydi, J. N. Eckstein, S. D. Bader, and J.-M. Zuo, Phys. Rev. Lett. **99**, 196404 (2007).
[30]R. I. Dass and J. B. Goodenough, Phys. Rev. B **67**, 014401 (2003).
[31]J. Gazquez, S. Bose, M. Sharma, M. A. Torija, S. J. Pennycook, C. Leighton, and M. Varela, APL Mater. **1**, 012105 (2013).